Design of a supply chain network for chemicals from biomass using green electrochemistry

Motahareh Kashanian, Sarah M Ryan*

Department of Industrial and Manufacturing Systems Engineering, Iowa State University, Ames, IA, USA

Abstract

Increasing concern about the environmental impact of industrial activities has prompted a shift to renewable energy sources and the development of environmentally conscious supply chains. In this regard, electrochemistry has shown promise for converting biomass into specialty chemicals in distributed facilities that exploit renewable energy resources. To examine the impact of electrochemistry technology on optimal supply chain configuration, we formulate a mixed-integer linear programming model to optimize the locations and capacities of distributed facilities for converting biomass to chemicals. The economic objective of the supply chain design model is to minimize the total annual cost of producing chemicals from biomass-derived glucose and delivering them to market. To analyze the trade-off between environmental and economic considerations, we also consider an environmental objective of minimizing greenhouse gas (GHG) emissions. The results of a US case study indicate that, while cost is minimized by constructing one large facility, GHG emissions are lowered by a distributed configuration. Varying the setting of a process design parameter expands the Pareto frontier along which decision-makers can choose a configuration according to their preferences between economic and environmental criteria.

Keywords: Chemical supply chain, Supply chain network design, Mixed-integer programming, Electrochemistry.

1. Introduction

In recent years, the environmental advantages of biomass have been rapidly transforming the prospects for its widespread use as a feedstock in chemical manufacturing, including for the production of commodity chemicals, which now relies heavily on finite fossil carbon resources. Biobased chemical production processes are designed to replace these non-renewable sources of carbon with sustainable carbon derived from diverse biomass feedstocks, such as carbohydrates, triglycerides, lignin, and proteins. To overcome some of the challenges associated with biomass substitution, researchers have proposed the development of platform intermediate compounds, aimed at simplifying the development of multiple chemical products (Shanks & Broadbelt, 2019). While it may remain a long-term goal to replace petrochemical processes with renewable electrosynthesis, the production of chemicals from biomass is already attainable through

E-mail addresses: smryan@iastate.edu (S.M. Ryan), motinaa@iastate.edu (M. Kashanian).

^{*} Corresponding author. Tel.:+1-515-294-4347

distributed electrochemical manufacturing (Harnisch & Urban, 2018). The electrochemical approach to biomass conversion, which has been underexplored, offers unique advantages. The technology utilizes electricity to access new reaction pathways. With this approach, biomass and waste carbon can be converted at lower temperatures with improved efficiency and with intermittent renewable electricity resources. Electrochemical methods enable a wide variety of chemical transformations, effluent treatment, and the conversion of complex organics into valuable hydrocarbons. They hold the potential for environmentally friendly and economically viable industrial processes via small-scale manufacturing (Akhade et al., 2020, Uno & Inada, 2018). Biomass in the US Midwest can be converted into a wide range of highly selective and on-demand products using electrochemistry. While not overstating the carbon footprint benefits associated with substituting biomass for petroleum feedstocks (Queneau & Han, 2022), it is important to investigate the potential improvement in the economic and environmental tradeoffs of distributed electrochemical manufacturing.

Adipic acid (AA) is one important commodity chemical that soon could be produced from biomass rather than petroleum feedstock in a clean process. This polymer, a building block central to the production of Nylon 6,6, is broadly used in food packaging, home goods (e.g., carpets), textiles and apparel, as well as in the automobile industry. However, the current production process of oxidizing fossil-based cyclohexane using concentrated nitric acid has many negative environmental effects, including high levels of greenhouse gas (GHG) emissions (Nicholson et al., 2021). One of the most promising alternative processes involves muconic acid, an emerging bio-based platform chemical. In this scheme, glucose produced from starch or cellulosic biomass is biologically converted to cis,cis-muconic acid (ccMA), which can then be converted to AA using precious metal catalysts and hydrogen gas (Rios et al., 2021). However, the hydrogen typically is derived from fossil methane through steam reforming. To overcome the use of natural gas, researchers also have explored electrochemical hydrogenation, a technology that can be powered using renewable electricity and that uses water as a source of hydrogen for the reaction. One of the recent successes is the electrochemical hydrogenation of ccMA to trans-3-hexenedioic acid (t3HDA), a potential substitute for AA as a precursor of performance-advantaged nylon (Matthiesen, Carraher, et al., 2016). Hybrid microbial electrosynthesis (HMES) integrates fermentation and electrosynthesis, enabling improved efficiency and productivity in industrial processes, with environmentally friendly, cost-effective operation (Dell'Anna et al., 2021). Several experiments showcased the capability to generate bioderived compounds without the requirement of separating or modifying the fermentation broth using HMES (Matthiesen, Suástegui, et al., 2016). That is, this electrochemical reaction can be performed directly in the fermentation broth, using its water and salts as an electrolyte, and eliminating the need for expensive separation and purification steps.

A similar process under development for AA would have the threefold benefit of using renewable biomass as a feedstock, relying on clean electricity to drive the reaction, and reducing waste by process intensification. In this study, we explore the potential of distributing this production among small-scale facilities to reduce transportation costs and related emissions while exploiting proximity to sources of clean energy.

To properly assess the economic and environmental sustainability of a manufacturing process, the scope of consideration must include issues arising in the supply chain from raw material suppliers to customers of the end product. Supply chain management integrates suppliers, manufacturers, distribution centers, and customers to facilitate the efficient transportation of materials from source to end-user, ensuring timely delivery, quality, and cost-effectiveness through coordinated product and information flow (Beamon, 1998). Supply chain design and optimization can benefit any industry or process, as it considers not only operations, but also business functionality and market dynamics (Laínez & Puigjaner, 2012). The strategic decisions in supply chain management refer to the high-level decisions and actions taken to design and manage an efficient and effective supply chain network. These decisions include supply chain structure, technology selection, facility capacities, and other factors that contribute to competitive advantage (Sharma et al., 2013). The design of the supply chain network, specifically considering the sizes and locations of distributed facilities, affects its profitability and environmental performance. An optimal design balances the scale economies of production facilities against proximity to sources of raw materials and inexpensive renewable energy sources.

Techno-economic analysis (TEA) is commonly used to assess the financial aspects of engineering endproducts and process designs, to provide investors with guidance on whether the processes and products
can be commercialized. Typically, the TEA is used to estimate a minimum selling price (MSP) to be used
as the unit price of a product in a break-even analysis (Scown et al., 2021). The analysis tends to focus
narrowly on the cost of building and operating a single production facility, ignoring the costs of transporting
raw materials inbound to the facilities and finished products outbound to customers. While this analysis is
a useful initial step towards assessing economic viability, it implicitly assumes that the MSP is obtained by
taking advantage of the scale economies associated with traditional production processes (but not shared
by electrochemical processes). It also ignores the potential economic and environmental benefits of locating
facilities close to sources of renewable energy.

To include a wider perspective, we formulate a mixed-integer linear program (MILP) to optimize the sizes and locations of distributed bio-based chemical production facilities that integrate fermentation with electrochemistry. Our bicriterion model considers two objectives to be minimized: the total annualized investment and operational cost, and the GHG emissions from transportation and electricity usage,

accounting for spatial variation in both the cost and emissions due to electricity obtained from the grid. We apply the model in a case study of the production of t3HDA from glucose in the US. The capital investment costs account for the disparities in economies of scale between the electrochemical reactor (ECR) and the other equipment. We examine different settings for the current density applied in the ECR, which affects both capital investment costs and electricity usage. We find that, in the Pareto frontier for each level of current density, the minimum cost solution features a single large facility while lower emission configurations distribute production across several smaller facilities. The consideration of alternative current densities generates an extended Pareto frontier in which the lowest current density generates the least GHG emissions while the highest current density considered results in the lowest annual cost.

The rest of this paper is organized as follows. The next section briefly reviews the relevant literature and describes the case study. The proposed mixed-integer linear programming model is elaborated in Section 3; it is then implemented for the case study in Section 4. Numerical results are presented and discussed in Section 5. Lastly, Section 6 offers some conclusions and suggestions for future research.

2. Literature Review and Application Specifics

Numerous studies, of which we highlight only a few, have been devoted to optimal design and operational planning of the biofuel supply chain. Ekşioğlu et al. (2009) introduced a MILP formulation to design and manage the supply chain for biomass-to-biorefinery, focusing on determining the ideal quantity, scale, and locations of facilities and biorefineries required for biomass processing. Huang et al. (2010) developed a mathematical model to minimize costs and meet demand, feedstock, and technology constraints by determining optimal locations, sizes, and capacities of biorefineries, as well as annual quantities of ethanol production, feedstock delivery, and ethanol delivery to demand cities. Supply chains for biomass-to-liquids were designed and planned optimally by You and Wang (2011) from an economic and environmental standpoint using a multi-objective, multiperiod MILP model taking into account alternative conversion pathways, technologies, biomass characteristics, and spatial distribution of demand. Murillo-Alvarado et al. (2015) showed that implementing a biorefinery system in Mexico using tequila industry residues offers substantial economic and environmental advantages, as demonstrated by their multi-objective optimization approach.

While much research is devoted to the use of biomass for fuels, Shekarian et al. (2022) found only a limited body of literature devoted to the design of supply chain networks for chemicals from biomass. Similarly, in a systematic review of the literature on sustainable supply chains using operations research techniques, only 7% of the works were set in the chemical industry (Barbosa-Póvoa et al., 2018). However, we can trace a thread of literature on the important role of environmental impacts in chemical supply chain

designs. Among the first researchers to integrate environmental factors into supply chain planning and design, Hugo and Pistikopoulos (2005) are considered pioneers. Their paper describes a mixed integer linear programming model for investment planning within a chemical supply chain that aims to address how to design and expand the capacity of facilities in an environmentally friendly manner. The mixed integer non-linear programming (MINLP) model proposed by Guillén-Gosálbez and Grossmann (2009) considers both economic and environmental objectives for chemical supply chains where emissions and feedstock requirements are uncertain. Gabrielli et al. (2020) studied the optimal design of low-carbon hydrogen supply chains considering multiple feedstocks and energy sources, including biomass, and developed a MILP algorithm to minimize costs and CO₂ emissions while meeting end-user demand.

The need for sustainable and environmentally friendly chemical production has prompted significant research and development in electrochemical synthesis technologies. According to Sulaymon and Abbar (2012), electrochemical technology presents a compelling solution for industrial processes, combining economic feasibility and environmental performance through its versatility, energy-efficiency, automation, and cost-effectiveness. Achieving successful implementation of electrochemical reactors relies on their design and scale-up. When scaling up and commercializing microbial electrochemical systems (MES) and related technologies, reducing capital costs is a vital economic consideration (Savla et al., 2021). A number of recent studies have investigated the relationship between cost and scale of electrochemical reactors. Sánchez and Martín (2018) noted that the commonly used six-tenths rule does not apply to small-scale, distributed facilities using this technology. Instead, they highlighted the linear relationship between electrolyzer capacity and cost, which significantly affected the overall equipment cost of renewable ammonia plants. The study by Perry et al. (2020) provided a comprehensive analysis of various reactor designs employed in electrochemical synthesis, ranging from small-scale setups to larger reactors. The review discussed the design, operation, and scaling of electrochemical cells as significant obstacles to the advancement and expansion of electrosynthesis. Guerra et al. (2020) found that the increase in the cost of electrolyzers becomes nearly linear as the capacity of the system increases. Based on the analysis of the selected papers, it can be concluded that the capacity and cost relationship of electrochemical reactors is approximately linear, corresponding to limited, if any, economies of scale.

2.1. Research Gap and Contribution

Few studies were found in the literature that simultaneously address the design of chemical supply chains from biomass with both economic and environmental objectives, along with considering a techno-economic analysis for a novel production process. Zhang et al. (2014) investigated the supply chain design for producing commodity chemicals from woody biomass to achieve optimal configurations of preprocessing hubs and biorefineries by determining their locations and capacities. In a case study of a

hypothetical scenario using forest residue as the feedstock in the US state of Minnesota, they also examined the trade-off between economic and environmental factors, specifically by minimizing GHG emissions. García-Velásquez et al. (2023) investigated the design of supply chains for biobased polyethylene terephthalate (PET), focusing on minimizing supply chain costs and environmental impact, developing a MILP and a life cycle optimization framework to analyze the trade-offs between economic and environmental factors. Our review of the literature identified the following gaps:

- Limited research on chemical supply chain design from biomass, with most studies focusing on biomass for fuels rather than chemical production.
- Limited consideration of techno-economic analysis for novel production processes in the design of chemical supply chains with multiple possible capacity levels of the facilities.
- Little investigation into the impact of electrochemical reactors on the overall supply chain design, including factors such as capacity, energy usage, GHG emissions, and transportation costs.

To address these gaps, we formulate a model to determine the locations and scale of distributed facilities including electrochemical reactors to produce chemicals from biomass-derived glucose, considering electricity usage, transportation, and market demand. We applied MILP with an exact solution to determine the Pareto-optimal points of our two-objective model, which exposes the tradeoff between minimizing the annual cost of the supply chain and reducing the GHG emissions associated with transportation and electricity usage. The facility investment and operating costs are based on a detailed technoeconomic analysis with various settings for the current density, a key technological parameter that affects both environmental performance and overall cost.

2.2. Case Study on t3HDA from Glucose

The schematic for the supply chain system to produce chemicals from biomass is shown in Figure 1. In this study, for simplicity, biomass is assumed to have already been converted to glucose. The plentiful large-scale milling facilities that form the first step of ethanol production from corn grain are a potential source of this raw material. Distributed integrated conversion facilities are assumed to be located adjacent to these ethanol plant mills, though each conversion facility may be supplied by multiple ethanol plants. Chemicals are then transported to demand zones. Rather than imposing a particular topological structure on the network, such as those studied by Ezaki et al. (2022), we assume that transportation routes exist from all suppliers to all candidate facility locations and from each of those locations to any customer.

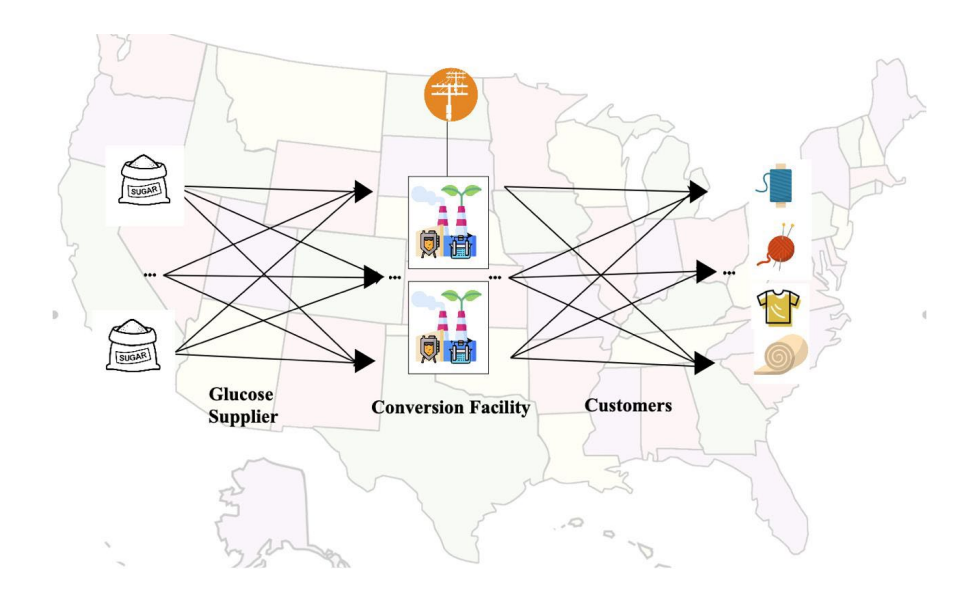


Figure 1. Supply chain schematic.

Ongoing investigations are being conducted into the techno-economics of scaling up and commercializing this process in light of the promising experimental results. A simplified analysis and determination of industrial feasibility had previously been performed with Early Stage Techno Economic Analysis (ESTEA) software (Matthiesen, Suástegui, et al., 2016). A further investigation was conducted by Dell'Anna et al. (2021) identifying cost breakdowns of this process for one large facility without considering the transportation costs, demand zones, supplier or facility location. Thus, the present work is necessary to outline a supply chain design for commercializing t3HDA production, taking into account the different possible capacities of the facilities and exploring the possibility of distributed manufacturing with the goal of minimizing costs and GHG emissions.

The current study examines the electrohydrogenation of ccMA to t3HDA in an electrochemical flow reactor and highlights parameters crucial to the design of a supply chain. Electrochemical reactors were given special consideration due to the fact that they represent the majority of utility costs and capital costs in the production process and do not follow the conventional economic scaling factors. It is important to note that for processes driven by heat, productivity scales with reactor volume, but for processes driven by electricity, productivity scales with reactor surface area. Consequently, conventional, heat-driven processes are better scaled up, while electrochemical reactors are best scaled out. In contrast to conventional heat-driven processes, where increasing a plant's capacity is more economical, electrochemistry is a promising technology for distributed chemical manufacturing (Pletcher & Walsh, 1993). Therefore, a trade-off between parameters related to technological aspects and supply chain configuration has been

investigated. The locations for the integrated conversion facilities are assumed to be the 197 ethanol plants in the US. The cost and greenhouse gas emissions per unit chemical produced are also quantified.

3. Mathematical Model Formulation

To design the supply chain for the production process illustrated in Figure 2, the objectives are to minimize the annual costs and GHG emissions associated with production and transportation based on the proposed production pathway of an integrated conversion facility. The deterministic bi-objective mixed integer linear programming model is defined using the notation summarized in Table 1.

Table 1. Notation for supply chain design mixed-integer programming model.

Sets	
J	Candidate facility locations, indexed by subscript <i>j</i>
K	Consumer centers, indexed by subscript <i>k</i>
С	Possible capacity levels of a facility, indexed by subscript <i>c</i>
Μ	Glucose suppliers, indexed by subscript <i>m</i>
B	Chemical production steps, indexed by superscript $b = F$ (fermentation), L
	(electrochemical reaction), S (separation) or P (purification)
Technical pa	
D_k	Demand of consumer center k for product (tonne/year)
r	Annual interest rate
N	Life of the facility in years
α	Tonnes of glucose needed/tonne of chemical produced
U_c	Capacity of integrated facility with capacity level c (tonne/year)
S_m	Capacity of supplier <i>m</i> (tonne/year)
W^b	Electricity requirement of production stage $b, b \in B$, per unit of production (kWh/tonne)
d_{uv}	Distance between supplier $u=m$ and facility location $v=j$ or between facility location $u=j$
α_{uv}	and customer $v=k$ (miles)
Cost parame	
V_g	Cost of glucose (\$/tonne)
K_{jc}^{b}	Fixed capital investment cost of stage $b, b \in B$, at location j , at capacity level c (\$)
V_j^{W}	Variable wastewater treatment cost at location <i>j</i> (\$/tonne)
$\overset{,}{V_j^L}$	Variable labor cost to produce chemical at location j (\$/tonne)
O_{jc}^{L}	Annual labor cost assuming a facility at location j , with capacity level c , is fully utilize
ŕ	(\$/year); equal to $V_i^L U_l$
$V_j^{UT.b}$	Variable non-electricity utility cost of stage $b, b \in B$, at location j (\$/tonne)
R_i	Variable cost of electricity at location <i>j</i> (\$/kWh)
T_{uv}	Transportation cost of glucose from supplier $u=m$ to location $v=j$ or chemical from location
¹ uv	$u=j$ to consumer center $v=k$ (\$\forall tonne-mile)
ϕ_1	Multiplier of capital investment cost to account for annual maintenance and repair
Ψ1	operating supplies, taxes and insurance, and a portion of plant overhead
ϕ_2	Multiplier of annual labor cost to account for annual administration costs and a portion
Ψ2	plant overhead
ϕ_3	Multiplier of variable labor cost to account for supervisory and clerical labor as well
Ψ3	laboratory charges
Environmen	ital parameters
E_j^G	GHG emissions from generation of electricity used at location j (kg CO ₂ equivalent per
-,	kWh)
E^T	GHG emissions of transportation (kg CO ₂ equivalent per tonne-mile)

Binary decis	sion variables
t_{jc}	1 if location j is selected for opening an integrated facility at capacity level c ; 0 otherwise
Continuous	decision variables
x_{uv}	Amount of glucose transported from supplier $u=m$ to facility location $v=j$ or chemicals
	transported from location $u=j$ to consumer center $v=k$ (tonne/year)
y_i	Amount of chemical produced at location <i>j</i> (tonne/year)
f_j	Amount of electricity used at location j (kWh/year)

In terms of the above notation, the problem can be formulated as follows.

3.1. Objective functions

Two important and conflicting objective functions are considered: (1) minimization of the total cost and (2) minimization of the total GHG emissions.

3.1.1. First objective: minimizing the total cost.

The total cost of the chemical supply chain network design includes the capital investment costs of establishing integrated facilities with four different processing stages of fermentation, electrochemical reaction, separation, and purification, along with the fixed and variable operational costs. The operational costs include variable cost of labor, raw materials, wastewater, transportation costs, and electricity costs that are dependent on the quantity of production. According to Turton et al. (2008), manufacturing costs include direct manufacturing costs, which vary according to the level of production; fixed manufacturing costs, such as property taxes and insurance, that are independent of production levels; and general expenses covering overhead expenses for critical business functions. Considering the capital investment costs of establishing integrated facilities, along with these operational costs, the annual cost objective function (\$/year) can be formulated as follows.

$$Min Z_{1} = \left[\left(\frac{r(1+r)^{N}}{(1+r)^{N}-1} \right) \sum_{c \in C} \sum_{j \in J} \sum_{b \in B} K_{jc}^{b} + \sum_{c \in C} \sum_{j \in J} \left(\sum_{b \in B} \phi_{1} K_{jc}^{b} + \phi_{2} O_{jc}^{L} \right) \right] t_{jc}$$

$$+ \sum_{j \in J} \left(\sum_{b \in B} V_{g} + V_{j}^{W} + V_{j}^{UT.b} + (1+\phi_{3}) V_{j}^{L} \right) y_{j} + \sum_{m \in M} \sum_{j \in J} T_{mj} d_{mj} x_{mj}$$

$$+ \sum_{j \in J} \sum_{k \in K} T_{jk} d_{jk} x_{jk} + \sum_{j \in J} R_{j} f_{j}$$

$$(1)$$

The first term in the cost objective function consists of annualized capital investment cost for establishing facilities, as well as the annual fixed manufacturing costs and general expenses. The second term comprises the direct manufacturing costs associated with the annual production of chemicals. The third and fourth terms account for the costs of transporting raw materials and final products, respectively. The costs of

transportation from glucose suppliers to the facilities and from production facilities to the demand zones are calculated by multiplying shipping distance by transportation cost per unit of distance (i.e., one mile) via truck in the US. The final term is the cost of electricity usage, which is distinguished from the other utility costs to facilitate the study of the impact of various current densities in the electrochemical reactors. Considering electricity usage separately also allows us to account for spatial variations in GHG emissions from electricity generation.

3.1.2. Second objective: minimizing the GHG emissions. The second objective function can be formulated as follows:

$$Min Z_2 = E^T \sum_{j \in J} \sum_{m \in M} d_{mj} x_{mj} + \sum_{j \in J} E_j^G f_j + E^T \sum_{k \in K} \sum_{j \in J} d_{jk} x_{jk}$$
(5)

Here we account for GHG emissions associated with transportation of glucose to the facilities, generation of the electricity used, and transportation of the final product to customer centers. Note that we measure GHG emissions in a manner similar to the demand-based carbon intensity indicator proposed for international shipping (Wang et al., 2021).

3.2. Constraints

3.2.1. Demand satisfaction constraints. Constraints (6) and (7) ensure that the demands of all consumer centers are satisfied, and all production is delivered.

$$\sum_{i \in I} x_{jk} = D_k, \quad \forall k \tag{6}$$

$$\sum_{k \in K} x_{jk} = y_j , \forall j \tag{7}$$

3.2.2. Flow balance constraints. In Constraint (8), the amount of chemicals produced is balanced with the amount of glucose based on the yield of the process. Constraint (9) computes the total amount of electricity required for the operations of each unit.

$$\sum_{m \in M} x_{mj} = \alpha y_j , \forall j$$
 (8)

$$\sum_{j \in I} f_j = \sum_{b \in B} W_j^b y_j , \forall j$$
(9)

3.2.3. Capacity constraints. The following are all relevant production capacity constraints. Constraint (10) prevents each facility from producing more chemicals than its capacity allows. As a result of constraint (11) at most one capacity level can be selected for a facility established at location *j*. Each supplier's capacity limit is enforced by constraint (12).

$$y_j \le \sum_{c \in C} U_c t_{jc} , \quad \forall j \tag{10}$$

$$\sum_{c \in C} t_{jc} \le 1, \quad \forall j \tag{11}$$

$$\sum_{i \in I} x_{mj} \le S_m, \quad \forall m \tag{12}$$

3.2.4. Variable restrictions. The following constraints specify the binary and non-negativity restrictions on the corresponding decision variables.

$$t_{ic} \in \{0,1\}, \qquad \forall j, c \tag{13}$$

$$x_{mi}, x_{jk}, y_i, f_i \ge 0, \qquad \forall m, j, k \tag{14}$$

3.3. The proposed solution method for two-objective model

Several approaches have been developed in the literature to solve multi-objective programming models. The ε-constraint method provides a picture of the whole Pareto-optimal solution set for the decision maker, allowing them to select their most preferred solution. Due to comprehensive information available, the decision maker can determine the final decision more confidently based on all possible solutions. Readers interested in learning more about this method may refer to (Ehrgott, 2005).

By expressing one objective as a constraint, the ε -constraint technique reduces a multi-objective problem to a single-objective problem. In this research, GHG emission is the ε -based constraint, and the higher priority function, total cost, is retained as the objective function. The reformulated problem is:

$$\begin{aligned}
Min Z &= Z_1 \\
s. t.
\end{aligned} \tag{15}$$

$$Z_2 \le \varepsilon$$
, Constraints (6)-(14)

Following is a general description of the process to identify the Pareto frontier of nondominated solutions. First, the ε -constraint on Z_2 in (16) is relaxed to find a minimum cost solution. The value of Z_2 in this solution is an upper bound on GHG emissions. Second, by reversing the roles of Z_1 and Z_2 in (15)-(16) and relaxing the resulting ε -constraint on Z_1 , a lower bound on GHG emissions is identified. Finally, the single objective problem originally written as (15)-(16) is solved by setting ε to discrete values evenly spaced

between the lower and upper bounds. The Pareto curve is thus approximated, showing the trade-off between economic and environmental objectives.

4. Case Study

4.1. TEA and cost analysis of chemical process

In the proposed chemical production process, ccMA is produced through fermentation of glucose, and then electrochemically converted into t3HDA. The novel unsaturated monomer t3HDA has enjoyed increased interest due to its ability to replace AA in Nylon 6,6 and produce polyamides with performance advantages. Low productivity has prevented t3HDA from being applied to the production of advanced polymers. A new synergy between microbial and electrochemical conversions was presented by Dell'Anna et al. (2021) for increasing t3HDA productivity by over 50 times. A process schematic is shown in Figure 2.

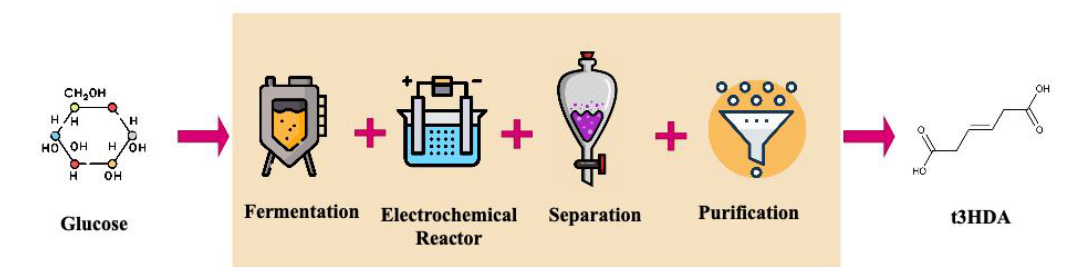


Figure 2. Chemical conversion process schematic.

In spite of the fact that no commercial, scaled up example has been found of a hybridized process that combines fermentation with electrochemistry, an analysis using ESTEA software demonstrated the scalability of t3HDA from bioderived ccMA (Matthiesen, Suástegui, et al., 2016). The ESTEA calculates the MSP by dividing total annual costs (\$/yr) by total annual production (kg/yr). Through the experimental design conducted by Dell'Anna et al. (2021), using Aspen software, an industrial design for converting glucose to MA by biological fermentation subsequent to electrochemical hydrogenation to t3HDA was modeled in detail, allowing for a more thorough TEA. The study focused solely on one large facility and overlooked the potential for multiple distributed facilities, did not consider the limited cost advantages of electrochemical reactors at smaller scales, and performed only a partial optimization of current density in the electrochemical reactor based on a single facility. In our study, we extracted valuable information from (Dell'Anna et al., 2021). We obtained the following key details:

- 1. The capacity of the base size (*c*=1) plant is 75,296 tonnes/year of t3HDA, based on the AA market as a reference.
- 2. It was assumed that the chemical plant operated for 8,000 hours per year.
- 3. The values of technical parameters such as α and W^n were derived from the Aspen flowsheet.
- 4. Equipment sizes for the base size plant were determined based on the output of the Aspen software, while its capital investment and manufacturing costs were calculated using CAPCOST.

To estimate additional parameter values for our supply chain design model, it was necessary to extract intermediate findings from this research and scale costs for various plant sizes. As part of our assessment, we analyzed both the operational manufacturing costs and the capital investment costs. Capital investment costs, also known as grass-roots costs, comprise the expenses incurred in constructing a new plant. These costs are made up of three main components: the total bare module capital cost, contingency and fee expenses, and auxiliary facilities costs. The total bare module capital cost encompasses the costs linked to each piece of equipment required for the plant. Contingency and fee costs are included to account for unexpected circumstances and contractor fees and are usually calculated as a percentage of the total module capital cost. Meanwhile, auxiliary facilities costs cover expenses such as land acquisition and electrical systems, and generally amount to about 30% of the total basic module cost, which includes the total bare module capital cost and contingency and fee expenses (Turton et al., 2008). The third column of Table 2 presents the fixed capital investment for each unit operation based on CAPCOST equipment costs for capacity level c=1 extracted from (Dell'Anna et al., 2021).

Table 2. Fixed capital investment (FCI, in \$M) by unit operation.

Model Notation	Stage of Production	Base Size $(c = 1)$	Half Size $(c = 2)$	Quarter Size $(c = 3)$
U_c	Capacity (tonne/year)	75,296	37,648	18,824
K^F_{jc}	Fermentation	10.86	7.17	4.73
K^L_{jc}	Electrochemical reactor	33.50	16.75	4.17
K^{S}_{jc}	Separation	1.71	1.13	0.74
K_{jc}^P	Purification	9.07	5.99	3.95
	Total FCI	55.15	31.03	17.80

To calculate the capital cost for smaller capacities in the table, we use the following equation:

$$K_{ic}^{n}/K_{i1}^{n} = (U_{c}/U_{1})^{p} (17)$$

where p represents the exponent or proration factor, the slope of a logarithmic curve that illustrates the cost change of a plant as it is scaled up or down. These curves are typically derived from known cost data of completed plants. In chemical plants, the exponent varies by type of equipment from 0.5 to 0.85 (Turton et al., 2008) but, as a default, is assumed to be 0.6 (the so-called "six-tenths rule"). As a result, we applied this value of p to all unit operations except the electrochemical reactor, for which we assume the size and capital cost scale linearly with capacity (i.e., p=1).

According to Turton et al. (2008), the total manufacturing cost consists of three categories: direct (variable) manufacturing costs, indirect manufacturing costs, and general expenses, where the latter two categories are fixed costs. Raw material expenses, catalyst and solvent costs, operating labor fees, supervisory and administrative labor fees, utilities (including waste disposal), maintenance and repairs, operating supplies, laboratory fees, patent and royalty payments, among others, are included in direct production costs. This category includes all fees for materials and labor. From the Aspen simulation results in (Dell'Anna et al., 2021), raw material and wastewater costs are calculated according to their flowrate. Accordingly, in the case of a continuously operating plant, it was assumed that 18 operators worked on average 8000 hours each year and that there were three shifts each day. The salary of the operator was estimated to be \$52,000 per year. In order to use it in our model, we calculate the cost of labor in terms of dollar per tonnes, and dollar per year for different plant capacities. According to CAPCOST sheet modeled by Dell'Anna et al. (2021), wastewater would cost around \$278.80 per tonne. According to Aspen's output modeled by Dell'Anna et al. (2021), the flowrate of glucose is 22019.5 kg/hr, which would result in annual raw material cost of \$53,151,360. A summary of the parameters is shown in Table 3.

Table 3. Variable costs of production.

Model Notation	Cost (\$/tonne)
V_j^L	37.29
V_j^W	278.80
V_{g}	705.90
$\sum_{b \in B} V_j^{UT.b}$	92.82

As shown in Table 4, other expenses, such as supervisory and clerical labor fees, maintenance and repair costs, and operating supplies charges, are calculated separately and multiplied by associated factors. Overhead, insurance, and local taxes are included in fixed manufacturing costs as these items are not

affected by the production rate of a plant. Finally, we have included administrative costs as part of the general expenses category. Distribution and selling costs, as well as research and development charges, are omitted because they do not vary with supply chain configuration. Table 4 summarizes the items related to manufacturing expenses commonly used in economic assessments (Turton et al., 2008).

Table 4. Manufacturing costs (\$M/yr) by facility size for current density 200 mA/cm².

Model Notation		Base Size $(c = 1)$	Half Size $(c = 2)$	Quarter Size $(c = 3)$
Direct Manuf	acturing Costs			
$V_g U_c$	Raw Material	53.15	26.57	13.29
$V_j^W U_c$	Waste Treatment	20.99	10.50	5.25
$V_j^L U_c$	Operating labor	2.81	1.40	0.70
$\sum_{b \in B} V_j^{UT.b} \ U_c$	Utilities (other than electricity)	6.99	3.49	1.75
$0.18O_{jc}^{L}$	Supervisory and clerical labor, 18% of operating labor	0.50	0.25	0.13
$0.06\sum_{b\in B}K_{jc}^{b}$	Maintenance and repairs, 6% of Fixed Investment Cost	3.31	1.86	1.07
$0.009 \sum_{b \in B} K_{jc}^b$	Operating supplies, 0.9% of Fixed Investment Cost	0.50	0.28	0.16
$0.15O_{jc}^L$	Laboratory charges, 15% of annual operating labor	0.42	0.21	0.10
Fixed Manufa	acturing Costs			
$0.7080_{jc}^{L} + 0.036 \sum_{b \in B} K_{jc}^{b}$	Plant overhead, 70.8% of operating labor + 3.6% of Fixed Investment Cost	3.97	2.11	1.14
$0.032\sum_{b\in B}K_{jc}^{b}$	Local taxes and Insurance, 3.2% of Fixed Investment Cost	1.76	0.99	0.57
General Man	ufacturing Expenses			
$0.1770_{jc}^{L} + 0.009 \sum_{b \in B} K_{jc}^{b}$	Administrative costs, 17.7% of operating labor + 0.9% Fixed Investment Cost	0.99	0.53	0.28
Total product	ion cost	95.40	48.21	24.44

By combining terms in Table 4, we find the value of the capital investment cost multiplier, $\phi_1 = 0.06 + 0.009 + 0.036 + 0.032 + 0.009 = 0.146$. The multiplier for annual labor cost to estimate fixed manufacturing costs and general expenses is $\phi_2 = 0.708 + 0.177 = 0.885$, while the multiplier for variable labor cost to include in direct manufacturing costs is $\phi_3 = 0.18 + 0.15 = 0.33$.

We obtained the electricity usage from (Dell'Anna et al., 2021), which was calculated based on the CAPCOST equipment sheet, and we calculated the consumption per tonne for each unit operation to use it in our model. Table 5 summarizes these parameter values.

Table 5. Electricity usage by production stage for current density 200 mA/cm² (Dell'Anna et al., 2021).

Model Notation	Stage of Production	Usage (kWh) per tonne
W^F	Fermentation	442.95
W^L	Electrochemical Reactor	2101.90
W^S	Separation	1.84
W^P	Purification	3.14
Total		2549.86

The transportation cost was calculated based on the assumption that trucks will transport both the glucose and the final product. The cost of a truck per mile is \$1.86, and each truck can transport 36.2874 tonnes. Based on this assumption, the transportation cost per mile was computed to be \$0.05.

In the US, commercial fuel ethanol is produced mainly by breaking down corn starch into simple sugars (glucose). Glucose is then fed to yeast for fermentation, resulting in the main product, ethanol, along with byproducts. Two major industrial methods used for ethanol production are wet milling and dry milling, where corn is processed through a hammer mill to produce corn flour from which the glucose is derived (DOE, July, 2023). The production of ethanol relies on fermentation, where yeast consumes glucose and generates carbon dioxide and ethanol as byproducts. It is estimated that for every pound of glucose, fermentation can produce about 1/2 pound (equivalent to 0.15 gallons) of ethanol (Mosier & Ileleji, 2020). We made the assumption that each US ethanol plant could divert up to 5% of its glucose capacity from the milling process as a feedstock for the production of t3HDA. To calculate the tonnage of glucose, we converted the capacity of each plant (measured in Mmgal/yr) into tonnes by multiplying them by 3081.84 tonne/Mmgal. This conversion was based on the density of ethanol, which is approximately 6.79434 lbs/gal (TheEngineeringToolBox).

For each US state containing an ethanol plant (thus, a potential location for distributed t3HDA production) we extracted greenhouse gas emissions per kilowatt hour of grid electricity from (U.S. Environmental Protection Agency, 2021) and the electricity rate from (EIA, February 2023 and 2022) as shown in Table 6 along with details regarding the 197 US ethanol plants and their corresponding assumed glucose capacities in 23 states.

Table 6. Glucose supply and electricity grid characteristics by US state.

_		11 /	, &		
		No. of		CO amission	Industrial
	State	Ethanol	5% of glucose capacity (Mtonne/year)	CO ₂ emission	Electricity rate
		Plants		rate (kg/kWh)	(\$/kWh)
_	Arizona	1	0.34	0.33	0.07

California	5	1.40	0.22	0.16
Colorado	3	0.86	0.55	0.08
Idaho	1	0.37	0.12	0.06
Illinois	12	10.72	0.30	0.08
Indiana	14	7.97	0.74	0.09
Iowa	42	28.77	0.35	0.06
Kansas	13	3.71	0.38	0.09
Kentucky	2	0.33	0.78	0.07
Michigan	6	2.70	0.45	0.08
Minnesota	19	8.66	0.37	0.09
Missouri	6	1.94	0.74	0.08
Nebraska	25	14.10	0.51	0.07
New York	2	1.00	0.21	0.07
North Carolina	- 1	0.35	0.30	0.07
North Dakota	5	3.25	0.61	0.07
Ohio	7	4.58	0.55	0.08
Oregon	1	0.25	0.15	0.07
Pennsylvania	1	0.79	0.33	0.08
South Dakota	16	8.79	0.14	0.08
Tennessee	3	1.45	0.32	0.07
Texas	4	2.50	0.39	0.07
Wisconsin	9	3.62	0.58	0.08

4.2. Effect of current density

We examined the relation between electrochemical reactor parameters and costs in detail. A cost calculation of electrochemical hydrogenation of a fermentation broth containing ccMA at pH 7 has been done by taking into account the tradeoff between the cost of the electrochemical reactor and the Faradaic efficiency, yield, and productivity as a function of the current density based on (Dell'Anna et al., 2021). During a reaction time, Faradaic efficiency indicates how many electrons are transmitted to the target molecules (Liu et al., 2020). The yield, which represents the ratio of moles of product to reactant, is used to measure the efficiency of a reaction (Levenspiel, 1998). The productivity of the process is the amount of product formed per hour.

To examine the impact of current density on parameters associated with our proposed supply chain design, we must first understand some basic electrochemical concepts. During an electrochemical reaction, the voltage, or the energy available to transfer charge, causes the reaction. Two half-reactions, an oxidation, and a reduction, must develop a net-zero charge balance in an electrochemical reaction. An electrolyte transfers charge in electrochemical reactions at the anode and cathode. On the anode, oxidations take place, and on the cathode, reductions. In the process under study, hydrogenation of MA at the cathode produces t3HDA. The parameter values presented previously were based on the assumption of the current density of 200 mA/cm² identified by Dell'Anna et al. (2021) as optimal for a single large plant. A low voltage operation results in a high energy efficiency, while a high current density results in a high production rate.

Our first step in calculating electrochemical reactor costs is to determine how much MA is converted to t3HDA, which we call the reaction rate. The reaction rate is then converted to current (Amps). Electrochemical reactor fixed cost is determined by the electrode area, which in turn is determined by the current density. Further, the voltage times the current must be calculated to arrive at the amount of power needed for an electrochemical reactor. A summary of electrochemical cost calculation and related parameters is shown in Figure 3.

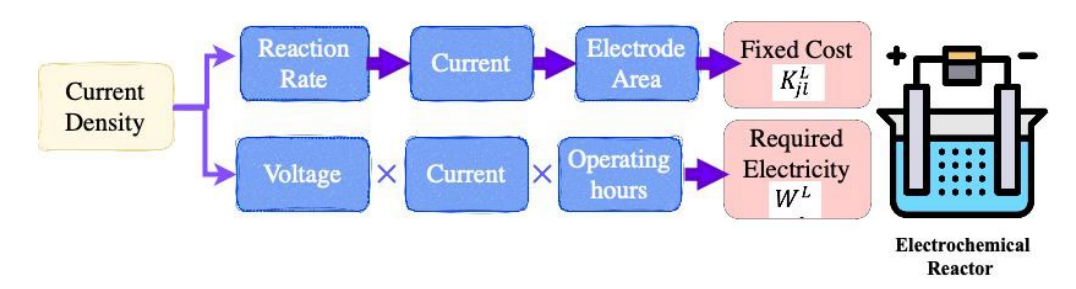


Figure 3. Electrochemical reactor cost and electricity usage.

Considering different parameters related to electrochemical reactors, we examine the cost of electrochemical reactors in different facility capacities shown in Table 7 to better understand how to design the supply chain for this process.

Table 7. Effect of current density on electricity usage and fixed capital investment for the large capacity electrochemical reactor.

Model	Current density (mA/cm ²)	50	200	400
Notation	Voltage (volts)	4	5.7	7.6
W^L	Electricity required per tonne, kWh	1475.02	2101.90	2802.53
K_{jc}^{L}	Total Capital Cost \$M	134.00	33.50	16.70

4.3. Supply chain design parameters

Since raw material costs make up a significant portion of the overall cost, we assume that facility candidate locations will be adjacent to a subset of the 197 US ethanol plants, in an effort to minimize the cost of transporting the raw materials. Glucose suppliers are also assumed to be ethanol plants. Demand is divided equally among the largest textile companies in the U.S (Mohawk Industries, Inc., Aladdin Div., Dalton, GA; Hanesbrands, Inc., Winston-Salem, NC; and Saint Gobain Tape Solutions, Hoosick Falls, NY (IndustrySelect)). Three different capacities are assumed for the integrated facilities based on the capacity estimate factor (Turton et al., 2008). The largest plant capacity is assumed to be 75296 tonne/year, or 3% of the approximate annual market size of adipic acid (the closest commercially available substance for t3HDA). Due to the economic benefits of distributed electrochemistry, the proposed supply chain design

also considers half and quarter of this size. For a period of 10 years, the total capital charge was amortized at 10% interest. This analysis ignored taxes, depreciation, and salvage values. Parameters with their values are summarized in Table 8.

Table 8. Summary of parameter values.

Notation	Definition		Value		
D_k	Demand of consumer center k for chemical	ls (tonne/year)	k=1, 25099 k=	2, 25099 k=	3, 25098
α	Tonnes of glucose needed/tonne of chemic	al produced	2.34		
			Base	Half	Quarter
		Stage of Production	Capacity	Capacity	Capacity
			(c = 1)	(c = 2)	(c = 3)
U_c	Capacity of single facility (tonnes/year)	All	75296	37648	18824
W^F	Variable electricity requirement (kWh/tonne)	Fermentation	442.97	442.97	442.97
W^L	Variable electricity requirement (kWh/tonne)	Electrochemical Reactor	2101.90	2101.90	2101.90
W^S	Variable electricity requirement (kWh/tonne)	Separation	1.84	1.84	1.84
W^P	Variable electricity requirement (kWh/tonne)	Purification	3.15	3.15	3.15
V_g	Cost of glucose (\$/tonne)	Fermentation	705.90	705.90	705.90
K_{jc}^F	Total capital investment cost (\$M)	Fermentation	10.86	7.17	4.73
K_{jc}^L	Total capital investment cost (\$M)	Electrochemical Reactor	16.70	8.35	4.17
K_{jc}^{S}	Total capital investment cost (\$M)	Separation	1.71	1.13	0.74
K_{jl}^{P}	Total capital investment cost (\$M)	Purification	9.07	5.99	3.95
V_j^W	Variable wastewater treatment cost (\$/tonne)	All	278.80	278.80	278.80
V_j^L	Variable labor cost (\$/tonne)	All	37.29	37.29	37.29
O^L_{jc}	Fixed labor cost (\$M/year)	All	2.81	1.4	0.70
$V_i^{UT.F}$	Variable utility cost (\$/tonne)	Fermentation	83.37	83.37	83.37
$V_j^{\mathit{UT.L}}$	Variable utility cost (\$/tonne)	Electrochemical Reactor	0	0	0
$V_i^{UT.S}$	Variable utility cost (\$/tonne)	Separation	4.39	4.39	4.39
$V_j^{UT.P}$	Variable utility cost (\$/tonne)	Purification	5.07	5.07	5.07
T_{uv}	Transportation cost of glucoses (\$/tonne-mile)	All	0.05	0.05	0.05
ϕ_1	Multiplier of capital investment cost	All	0.146	0.146	0.146
ϕ_2	Multiplier of annual labor cost	All	0.885	0.885	0.885
ϕ_3	Multiplier of variable labor cost	All	0.33	0.33	0.33

GHG emissions of transportation (kg
CO2/tonne-mile)

All
0.19
0.19

5. Results and discussion

 E^T

In this study we explore the electrohydrogenation of ccMA to t3HDA in an electrochemical flow reactor, as well as parameters crucial to the design of supply chains. We focused on electrochemical reactors because they account for the majority of utility costs and operational costs in the production process. In addition, they do not follow conventional economic scaling factors, and are best used in distributed production processes. As a result, a trade-off between technological aspects and supply chain configuration has been investigated. In this section, the validity of the developed model is investigated via the data withdrawn from the considered case study. To verify consistent results with the TEA previously performed, we first solve our model assuming only one facility without considering transportation costs. In the case of one facility, we solve the MILP with one base capacity (c = 1), one facility location (j = 1) and one demand zone (k1=75296 tonne/year), and we relax the supplier capacity constraint (12), as well as considering only an economic objective function without the transportation cost terms ($\sum_{m=1}^{M} \sum_{i=1}^{J} T_{mj} d_{mj} x_{mj} + \sum_{i=1}^{J} \sum_{k=1}^{K} T_{jk} d_{jk} x_{jk}$). Figure 4 summarizes the results.

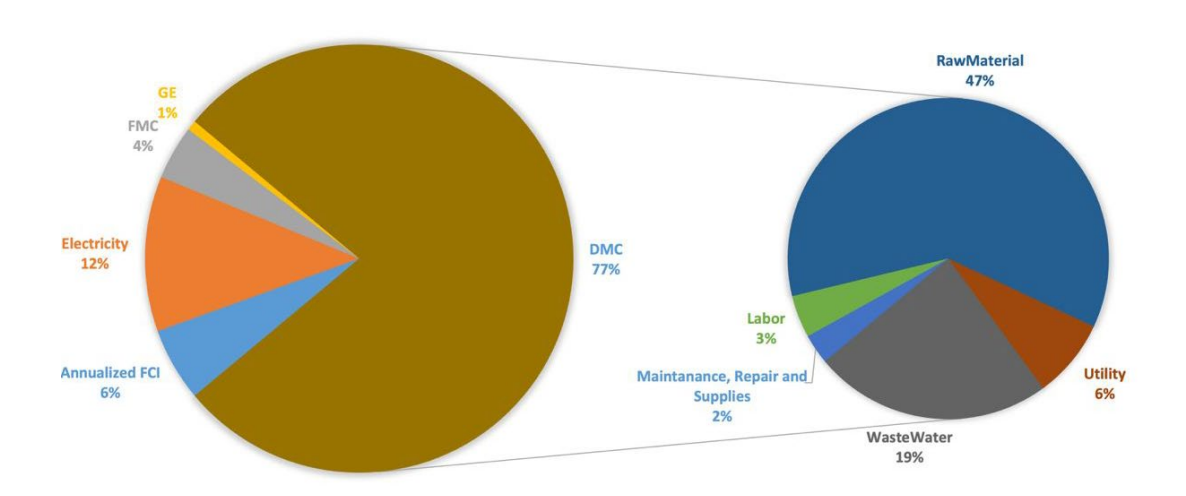


Figure 4. Cost breakdown for single facility.

All tests are conducted on the proposed model coded and solved by GAMS optimization software. A Pareto-optimal solution is generated by using the ε -constraint method described in Section 3.3. As we proceed, we discuss how supply chain design can be influenced by current density, whether it is better to distribute chemical facilities, or whether economies of scale can be beneficial.

5.1. Supply chain configuration based on current density 200 mA/cm²

To reduce the environmental impact of a supply chain design, it may be necessary to sacrifice some of its economic benefits in order to reduce transportation emissions and use renewable electricity more efficiently in a distributed manner instead of in a single large facility. Several supply chain structures and planning decisions are reflected in the set of Pareto points. With a tighter constraint on emissions, facilities become smaller and distributed in proximity to suppliers and demand zones, to reduce transportation emissions while satisfying all constraints related to the supply chain. Facility locations for each Pareto point are summarized in Table 9.

Table 9. Summary of Pareto points for current density 200 mA/cm².

Pareto Point	Facility Location	State	Facility Capacity	Cost Objective (\$M)	Emission Objective (M kg CO ₂ -eq)
1	Tate & Lyle	Tennessee	1	120.62	72.33
2	Tate & Lyle	Tennessee	2	122.04	50.22
2	Western New York Energy LLC	New York	2	122.04	58.33
	Western New York Energy LLC	New York	2		
3	Tate & Lyle	Tennessee	3	124.98	53.71
	Sioux River Ethanol	South Dakota	3		
	Western New York Energy LLC	New York	2		
	Sioux River Ethanol	South Dakota	3		
4	Attis Ethanol Fulton LLC	New York	3	137.81	47.64
	Northern Lights Ethanol LLC	South Dakota	3		
	Valero Renewable Fuels	South Dakota	3		

Figure 5 summarizes the supply chain components for each pareto point. Because ethanol plants are assumed to be the candidate locations for our facilities, some locations include both a glucose supplier and a facility. Facility locations tend to be in states with lower grid GHG emission rates as the supply chain configuration becomes more environmentally friendly.

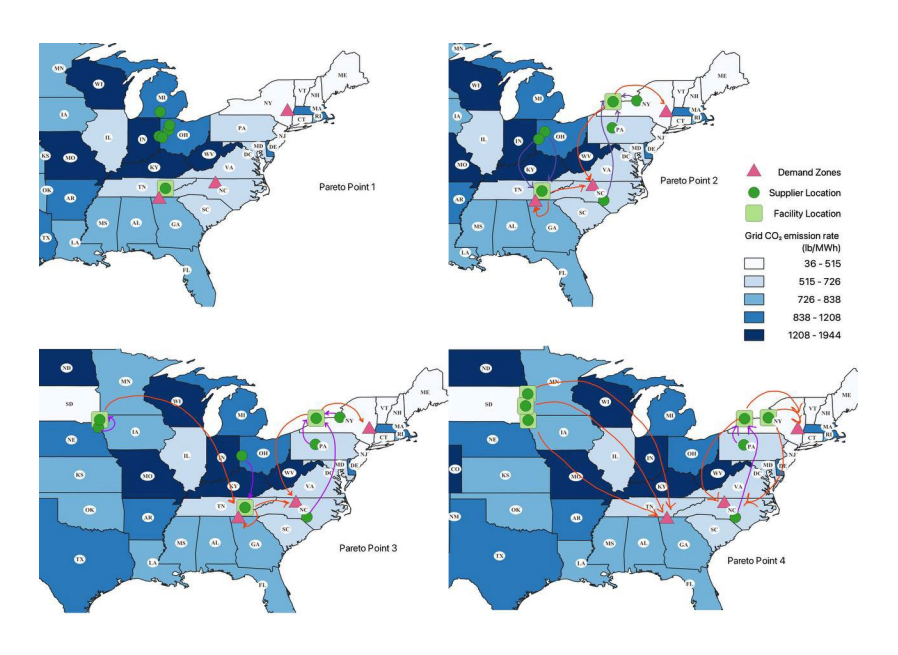


Figure 5. Supply chain configuration at Pareto points for current density 200 mA/cm².

5.2. Supply chain configuration based on current density 50 mA/cm²

Each Pareto point in the optimization process involves various supply chain structures and planning decisions. As with the baseline current density, by aiming to reduce emissions, facilities are designed to be smaller and strategically located near suppliers and demand zones. Table 10 summarizes the facility locations corresponding to each Pareto point.

Table 10. Summary of Pareto points for current density 50 mA/cm².

Pareto Point	Facility Location	State	Facility Capacity	Cost Objective (M\$)	Emission Objective (M kg CO ₂ -eq)
1	Tate & Lyle	Tennessee	1	148.39	57.38
2	Tate & Lyle	Tennessee	2	140.79	45.00
2	Western New York Energy LLC	New York	2	149.78	45.98
	Western New York Energy LLC	New York	2		
3	Tate & Lyle	Tennessee	3	151.51	42.96
	Sioux River Ethanol	South Dakota	3		
	Western New York Energy LLC	New York	2		
	Sioux River Ethanol	South Dakota	3		
4	Attis Ethanol Fulton LLC	New York	3	180.87	39.18
	Northern Lights Ethanol LLC	South Dakota	3		
	Valero Renewable Fuels	South Dakota	3		

Figure 6. summarizes the supply chain components for each Pareto point. Compared to the supply chain configuration based on current density 200 mA/cm², this one differs in the distribution of suppliers. For Pareto point 3 in this case, Michigan is also a supplier.

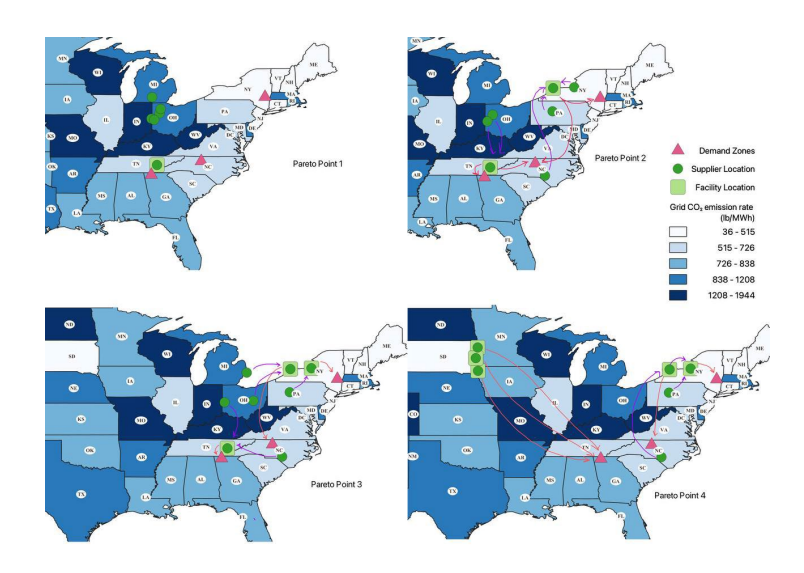


Figure 6. Supply chain configuration at Pareto points for current density 50 mA/cm².

5.3. Supply chain configuration based on current density 400 mA/cm².

Table 11 presents a summary of the Pareto points for a current density of 400 mA/cm², showcasing the facility locations, states, facility capacities, cost objectives (in million dollars), and emission objectives (in million kilograms of CO₂-equivalent). These Pareto points highlight the trade-offs between cost and emissions for different facility configurations. It is worth noting that this particular configuration, characterized by high electricity consumption, results in distinct Pareto points compared to two other configurations. Despite the possibility of constructing multiple smaller facilities, the Pareto points demonstrate the importance of balancing objectives when striving for optimal outcomes.

Table 11. Summary of Pareto points for current density 400 mA/cm².

Pareto Point	Facility Location	State	Facility Capacity	Cost Objective (M\$)	Emission Objective (M kg CO ₂ -eq)
1	Adm Clinton Ia	Iowa	1	118.71	104.22
2	Tate & Lyle	Tennessee	1	119.07	89.04
3	Adm Clinton Ia	Iowa	2	120.33	79.60
	Western New York Energy LLC	New York	2	120.33	
4	Western New York Energy LLC	New York	1	121.08	67.99
5	Western New York Energy LLC	New York	2		
	Sioux River Ethanol	South Dakota	3		
	Attis Ethanol Fulton LLC	New York	3	134.55	57.01
	Northern Lights Ethanol LLC	South Dakota	3		
	Valero Renewable Fuels	South Dakota	3		

As shown in Figure 7, this supply chain differs from two other supply chains in terms of the distribution of suppliers and the location of facilities. Due to the fact that, in this scenario, the most electricity is expected to be used, the model has attempted to locate the facilities in states with the lowest electricity rates in comparison with other states. To minimize environmental objective function, more distributed facilities tend to be located in states with lower grid emission rates, with suppliers and facilities located as near as possible to reduce transportation emissions as well.

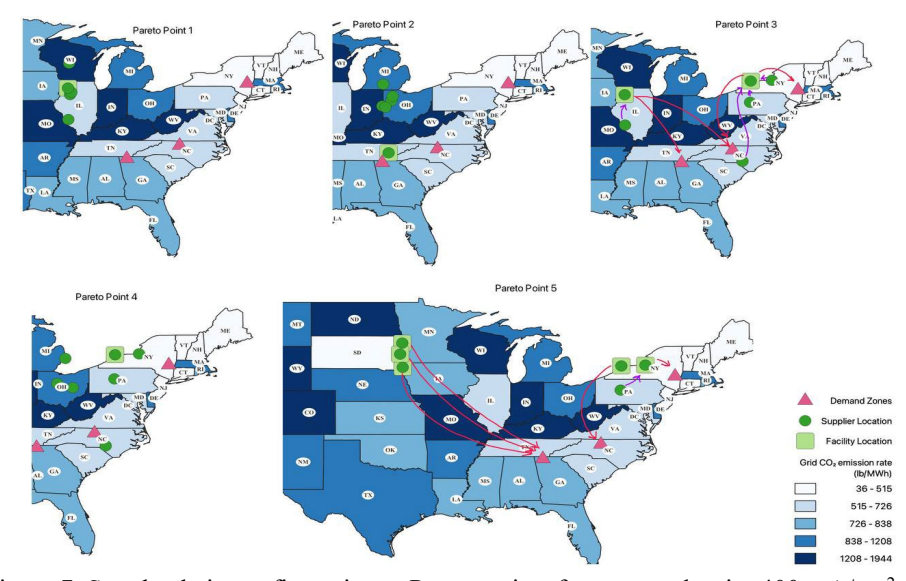


Figure 7. Supply chain configuration at Pareto points for current density 400 mA/cm².

5.4. Economic Perspective

The economic comparison among configurations is summarized in Table 12. Overall supply chain costs are dominated by the variable costs, especially raw materials. As a result, for this HMES process, optimal supply chain design is influenced more strongly by technology and process parameters than by economies of scale.

Table 12. Cost breakdown (\$M/y) of most economical supply chain configuration by current density.

Current Density (mA/cm²)	Annualized FCI	Fixed Production Costs	Variable Production Costs	Transportation Costs	Electricity cost (\$M/y)	Total costs of the supply chain configuration
						(\$M/y)
50	25.33	14.47	95.61	3.00	9.98	148.39
200	8.97	6.73	88.67	3.00	13.23	120.62
400	6.24	5.44	87.51	4.92	14.59	118.71

The cost breakdown analysis of the three cost-minimizing supply chain configurations based on different current densities reveals notable variations in the cost distribution. The annualized capital cost shows significant differences between the configurations. The configuration with a current density of 50 mA/cm² has the highest annualized capital cost of \$25.33M, while the configuration with a current density of 400 mA/cm² has the lowest annualized capital cost of \$6.24M. The configuration with a current density of 200 mA/cm² falls in between, with an annualized capital cost of \$8.97M. Variable production cost is relatively similar across the configurations, with the configuration based on a current density of 50 mA/cm² having the highest cost of \$95.61M. The configuration with a current density of 400 mA/cm² has the lowest cost at \$87.51, while the 200 mA/cm² configuration falls in between with a cost of \$88.67M. Because labor, raw material, utility, and wastewater costs remain constant across the configurations, the difference in variable costs is due to the components estimated as proportions of capital investment costs.

The electricity cost varies among the configurations. The highest electricity cost of \$14.59M occurs with the configuration based on the highest current density, while the lowest electricity cost of \$9.98M is achieved with the lowest current density. The costs associated with final transportation and glucose transportation are nearly the same for the lower current densities, but higher if the higher current density is used.

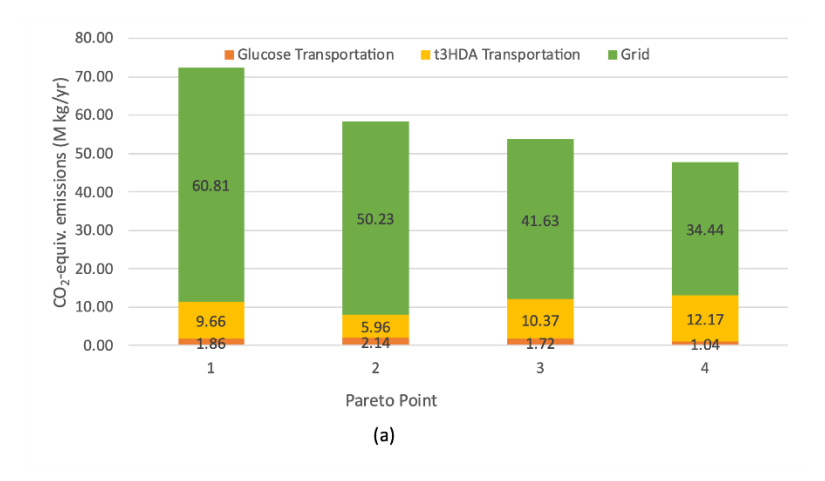
To summarize the cost breakdown analysis, the configuration with a current density of 400 mA/cm² has the lowest capital costs and fixed costs compared to the other configurations. However, it incurs the highest electricity cost. The configuration based on a current density of 50 mA/cm² has the highest fixed cost and lowest electricity costs. The 200 mA/cm² configuration falls between the other two configurations in terms of cost components.

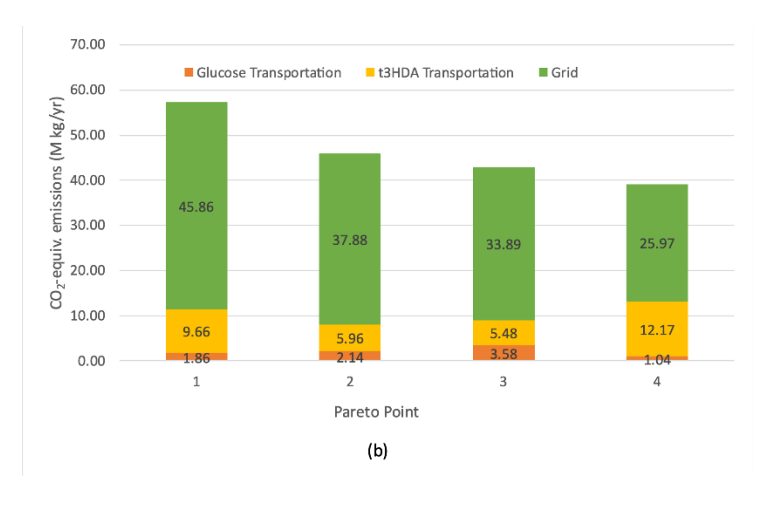
5.5. Environmental Perspective

The analysis of facility locations on different Pareto-optimal points for the various current densities studied provides insights into the optimal configurations based on cost and emission objectives. The facility locations vary across the Pareto optimal points for each current density. Multiple facilities from different states are identified as part of the optimal solution at each Pareto point. The cost and emission objectives differ for each Pareto-optimal point, reflecting the trade-off between minimizing costs and reducing emissions. Some facility locations appear consistently across multiple current densities, indicating their effectiveness in achieving Pareto optimality. For example, Western New York Energy LLC in New York and Tate & Lyle in Tennessee are found in the optimal solutions for all three current densities. The facility capacity remains the same within each Pareto optimal point, but the cost and emission objective values vary. This suggests that different configurations can achieve the same capacity while prioritizing either cost

reduction or emission reduction. Figure 8 illustrates a comparison between different CO₂-equiv. emissions (M kg/yr) by source for Pareto points with each value of the current density. The shifting distribution of emissions from various sources suggests that, to improve overall environmental performance, lowered emissions from electricity use are partially offset by increased emissions from transporting either the raw material or the finished product. However, there is no straightforward way to determine, without solving the optimization model, whether production facilities should be located closer to raw material sources or to customers.

The optimal facility locations are spread across different states, indicating the potential for regional distribution of the proposed chemical facility to optimize the supply chain. The Pareto curves obtained by following the proposed model in different cases can be seen in Figure 9.





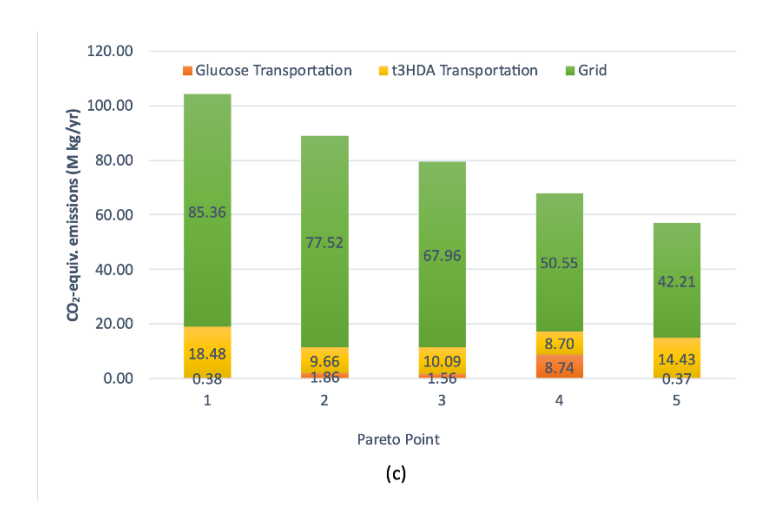


Figure 8. GHG emissions by source for the Pareto points with current density (a) 50 mA/cm², (b) 200 mA/cm², (c) 400 mA/cm².

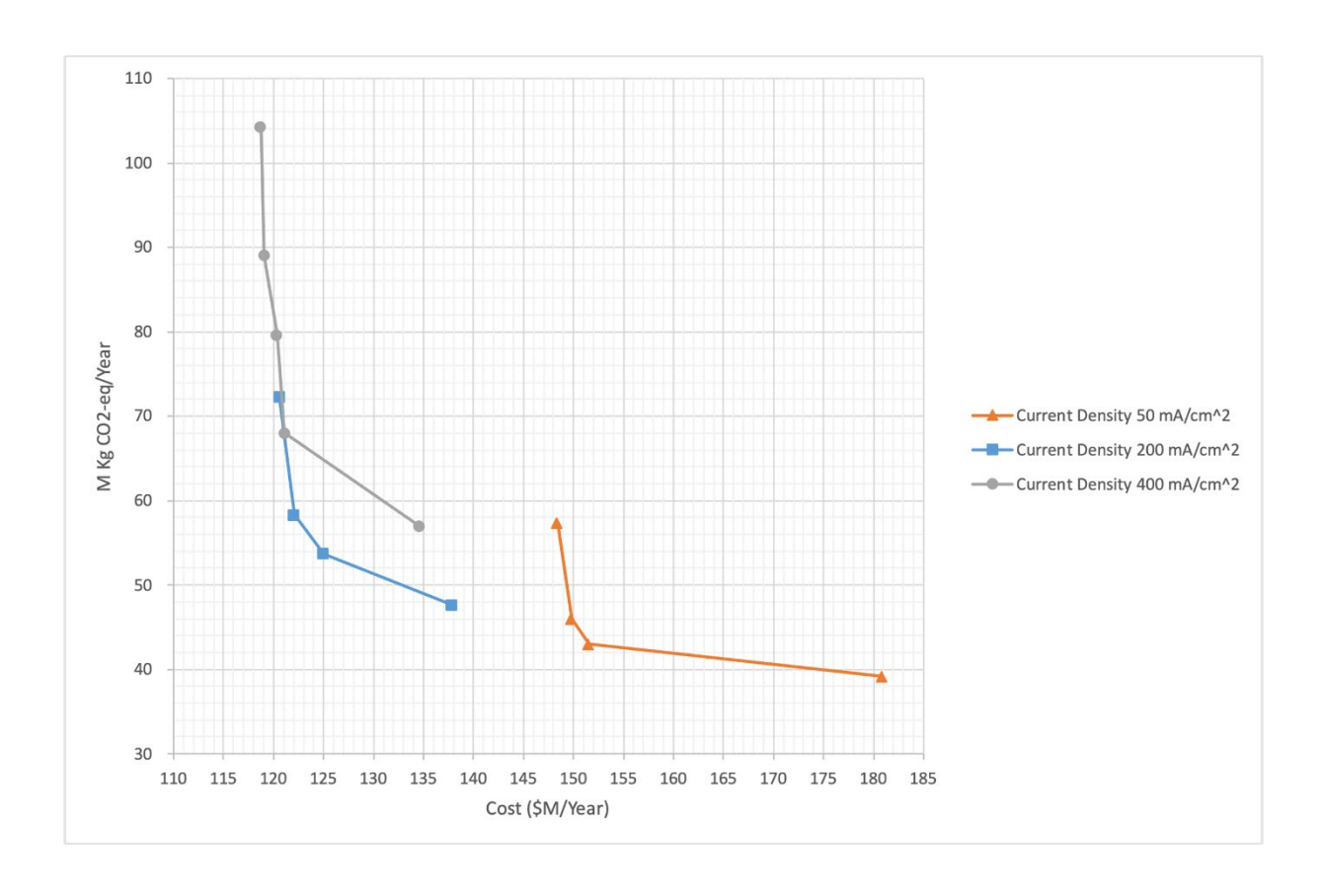


Figure 9. Pareto-optimal curves for various current densities.

Note that the lower envelope of the three Pareto curves forms a composite frontier of nondominated configurations, where the decision maker can select a current density according to the relative importance they attach to economic and environmental criteria. A lower current density would result in lower energy consumption, which would result in less CO₂ emissions, and a higher current density would result in lower costs, but more pollution.

6. Conclusions

Recent years have seen an increase in environmental concerns. Biological-electrochemical conversion of glucose to t3HDA has shown promising preliminary results, prompting further exploration of its technoeconomic feasibility and optimum supply chain configuration. Supply chain design is a complicated and important decision that should take environmental as well as economic concerns into account.

This paper presents a supply chain design considering feedstock availability, transportation, and market demand.

The case study on converting glucose into ccMA through biological fermentation to minimize operating costs for t3HDA production through electrochemical hydrogenation is based on data collected from real-life experiments. The technology of electrochemical reactors has been investigated at various capacity levels and configurations.

The results indicate that the absence of economies of scale in the electrochemical reactors increases the potential for small-scale production facilities to be located close to the sources of raw materials and where clean energy is more abundant. It was our objective to learn more about the cost parameters related to this novel part of the process and determine how they might affect supply chain design. The current density, which is one of the key parameters in electrochemical cost and productivity, has a significant impact on the supply chain's costs and emissions. Increased current density can reduce the energy efficiency of electrochemical reactors. However, the energy that is not utilized in an electrochemical reactor is diverted into hydrogen evolution, which we did not address in this study. Therefore, accounting for hydrogen production and exploring its potential applications, including its storage and subsequent use in fuel cells to help power the electrochemical reactor, represent promising avenues for future research. Ongoing experiments aim to enhance productivity and other aspects of this process. Additionally, we currently approximate the reaction rate as constant over time, but further investigations can explore its timedependent behavior for more accurate modeling. It would be worthwhile to revisit our assumption about the amount of glucose available to divert from ethanol production. Future research should take into account the upstream portion of this supply chain in greater depth. Moreover, the deterministic approach used in this study does not account for uncertainties in many parameters, including demand, which greatly influence

supply chain design geographically, economically, and environmentally. Future research should be conducted in an uncertain environment based on the findings of this study.

Acknowledgment

This material is based upon work supported by the National Science Foundation under Grants No. DGE-1828942 and EFMA-2132200. Thanks to Riley Hogan and Sarah Ng for their assistance in gathering cost and technical data, and JP Tessonnier for helpful discussions.

References

- Barbosa-Póvoa, A. P., da Silva, C., & Carvalho, A. (2018). Opportunities and challenges in sustainable supply chain: An operations research perspective. *European Journal of Operational Research*, 268(2), 399-431.
- Beamon, B. M. (1998). Supply chain design and analysis:: Models and methods. *International Journal of Production Economics*, 55(3), 281-294. https://doi.org/https://doi.org/10.1016/S0925-5273(98)00079-6
- Dell'Anna, M. N., Laureano, M., Bateni, H., Matthiesen, J. E., Zaza, L., Zembrzuski, M. P., Paskach, T. J., & Tessonnier, J.-P. (2021). Electrochemical hydrogenation of bioprivileged *cis,cis*-muconic acid to *trans*-3-hexenedioic acid: from lab synthesis to bench-scale production and beyond. *Green Chemistry*, 23(17), 6456-6468. https://doi.org/10.1039/d1gc02225c
- DOE, U. S. D. o. E. (July, 2023). *United States Department of Energy, Ethanol Production and Distribution*. https://afdc.energy.gov/fuels/ethanol-production.html
- Ehrgott, M. (2005). Multicriteria optimization. Springer Science & Business Media.
- EIA, F. (February 2023 and 2022). From EIA-861M (formerly EIA-826), Monthly Electric Power Industry Report. U.S. Energy Information Administration. Retrieved February 2023 and 2022 from https://www.eia.gov/electricity/monthly/epm table grapher.php?t=epmt 5 6 a
- Ekşioğlu, S. D., Acharya, A., Leightley, L. E., & Arora, S. (2009). Analyzing the design and management of biomass-to-biorefinery supply chain. *Computers & Industrial Engineering*, 57(4), 1342-1352.
- Ezaki, T., Imura, N., & Nishinari, K. (2022). Towards understanding network topology and robustness of logistics systems. *Communications in Transportation Research*, *2*, 100064. https://doi.org/https://doi.org/10.1016/j.commtr.2022.100064
- Gabrielli, P., Charbonnier, F., Guidolin, A., & Mazzotti, M. (2020). Enabling low-carbon hydrogen supply chains through use of biomass and carbon capture and storage: A Swiss case study. *Applied Energy*, 275, 115245. https://doi.org/https://doi.org/10.1016/j.apenergy.2020.115245
- García-Velásquez, C., Defryn, C., & van der Meer, Y. (2023). Life cycle optimization of the supply chain for biobased chemicals with local biomass resources. *Sustainable Production and Consumption*, 36, 540-551. https://doi.org/10.1016/j.spc.2022.10.015
- Guerra, C. F., Reyes-Bozo, L., Vyhmeister, E., Caparrós, M. J., Salazar, J. L., & Clemente-Jul, C. (2020). Technical-economic analysis for a green ammonia production plant in Chile and its subsequent transport to Japan. *Renewable Energy*, 157, 404-414.
- Guillén-Gosálbez, G., & Grossmann, I. E. (2009). Optimal design and planning of sustainable chemical supply chains under uncertainty. *AIChE Journal*, 55(1), 99-121. https://doi.org/https://doi.org/10.1002/aic.11662
- Harnisch, F., & Urban, C. (2018). Electrobiorefineries: Unlocking the Synergy of Electrochemical and Microbial Conversions. *Angewandte Chemie International Edition*, *57*(32), 10016-10023. https://doi.org/https://doi.org/10.1002/anie.201711727

- Huang, Y., Chen, C.-W., & Fan, Y. (2010). Multistage optimization of the supply chains of biofuels. *Transportation Research Part E: Logistics and Transportation Review*, 46(6), 820-830. https://doi.org/10.1016/j.tre.2010.03.002
- Hugo, A., & Pistikopoulos, E. N. (2005). Environmentally conscious long-range planning and design of supply chain networks. *Journal of Cleaner Production*, *13*(15), 1471-1491. https://doi.org/https://doi.org/10.1016/j.jclepro.2005.04.011
- IndustrySelect. *The Largest Textile Mills in the U.S.* Retrieved May, 2022 from https://www.industryselect.com/blog/10-largest-textile-mills-in-the-us
- Laínez, J. M., & Puigjaner, L. (2012). Prospective and perspective review in integrated supply chain modelling for the chemical process industry. *Current Opinion in Chemical Engineering*, *I*(4), 430-445. https://doi.org/https://doi.org/10.1016/j.coche.2012.09.002
- Levenspiel, O. (1998). Chemical reaction engineering. John Wiley & Sons.
- Liu, W., You, W., Gong, Y., & Deng, Y. (2020). High-efficiency electrochemical hydrodeoxygenation of bio-phenols to hydrocarbon fuels by a superacid-noble metal particle dual-catalyst system. *Energy & Environmental Science*, 13(3), 917-927.
- Matthiesen, J. E., Carraher, J. M., Vasiliu, M., Dixon, D. A., & Tessonnier, J.-P. (2016). Electrochemical Conversion of Muconic Acid to Biobased Diacid Monomers. *ACS Sustainable Chemistry & Engineering*, 4(6), 3575-3585. https://doi.org/10.1021/acssuschemeng.6b00679
- Matthiesen, J. E., Suástegui, M., Wu, Y., Viswanathan, M., Qu, Y., Cao, M., Rodriguez-Quiroz, N., Okerlund, A., Kraus, G., Raman, D. R., Shao, Z., & Tessonnier, J.-P. (2016). Electrochemical Conversion of Biologically Produced Muconic Acid: Key Considerations for Scale-Up and Corresponding Technoeconomic Analysis. *ACS Sustainable Chemistry & Engineering*, 4(12), 7098-7109. https://doi.org/10.1021/acssuschemeng.6b01981
- Mosier, N. S., & Ileleji, K. E. (2020). How fuel ethanol is made from corn. *Bioenergy*, 539-544.
- Murillo-Alvarado, P. E., Guillén-Gosálbez, G., Ponce-Ortega, J. M., Castro-Montoya, A. J., Serna-González, M., & Jiménez, L. (2015). Multi-objective optimization of the supply chain of biofuels from residues of the tequila industry in Mexico. *Journal of Cleaner Production*, 108, 422-441. https://doi.org/10.1016/j.jclepro.2015.08.052
- Nicholson, S. R., Rorrer, N. A., Carpenter, A. C., & Beckham, G. T. (2021). Manufacturing energy and greenhouse gas emissions associated with plastics consumption. *Joule*, *5*(3), 673-686. https://doi.org/https://doi.org/10.1016/j.joule.2020.12.027
- Perry, S. C., de León, C. P., & Walsh, F. C. (2020). The Design, Performance and Continuing Development of Electrochemical Reactors for Clean Electrosynthesis. *Journal of The Electrochemical Society*, 167(15), 155525.
- Pletcher, D., & Walsh, F. (1993). Industrial Electrochemistry.
- Queneau, Y., & Han, B. (2022). Biomass: Renewable carbon resource for chemical and energy industry. *The innovation*, *3*(1).
- Rios, J., Lebeau, J., Yang, T., Li, S., & Lynch, M. D. (2021). A critical review on the progress and challenges to a more sustainable, cost competitive synthesis of adipic acid. *Green Chemistry*, 23(9), 3172-3190. https://doi.org/10.1039/d1gc00638j
- Sánchez, A., & Martín, M. (2018). Scale up and scale down issues of renewable ammonia plants: Towards modular design. *Sustainable Production and Consumption*, 16, 176-192. https://doi.org/10.1016/j.spc.2018.08.001

- Savla, N., Suman, Pandit, S., Verma, J. P., Awasthi, A. K., Sana, S. S., & Prasad, R. (2021). Techno-economical evaluation and life cycle assessment of microbial electrochemical systems: A review. *Current Research in Green and Sustainable Chemistry*, *4*, 100111. https://doi.org/https://doi.org/10.1016/j.crgsc.2021.100111
- Scown, C. D., Baral, N. R., Yang, M., Vora, N., & Huntington, T. (2021). Technoeconomic analysis for biofuels and bioproducts. *Current Opinion in Biotechnology*, 67, 58-64. https://doi.org/https://doi.org/10.1016/j.copbio.2021.01.002
- Shanks, B. H., & Broadbelt, L. J. (2019). A Robust Strategy for Sustainable Organic Chemicals Utilizing Bioprivileged Molecules. *ChemSusChem*, 12(13), 2970-2975. https://doi.org/https://doi.org/10.1002/cssc.201900323
- Sharma, B., Ingalls, R. G., Jones, C. L., & Khanchi, A. (2013). Biomass supply chain design and analysis: Basis, overview, modeling, challenges, and future. *Renewable and Sustainable Energy Reviews*, 24, 608-627. https://doi.org/10.1016/j.rser.2013.03.049
- Shekarian, E., Ijadi, B., Zare, A., & Majava, J. (2022). Sustainable supply chain management: a comprehensive systematic review of industrial practices. *Sustainability*, *14*(13), 7892.
- Sulaymon, A. H., & Abbar, A. H. (2012). Scale-up of electrochemical reactors. *Electrolysis*, 17.
- TheEngineeringToolBox. *Ethanol Density and Specific Weight vs. Temperature and Pressure*. https://www.engineeringtoolbox.com/ethanol-ethyl-alcohol-density-specific-weight-temperature-pressure-d https://www.engineeringtoolbox.com/ethanol-ethyl-alcohol-density-specific-weight-temperature-pressure-d https://www.engineeringtoolbox.com/ethanol-ethyl-alcohol-density-specific-weight-temperature-pressure-d https://www.engineeringtoolbox.com/ethanol-ethyl-alcohol-density-specific-weight-temperature-pressure-d https://www.engineeringtoolbox.com/ethanol-ethyl-alcohol-density-specific-weight-temperature-pressure-d https://www.engineeringtoolbox.com/ethanol-ethyl-alcohol-density-specific-weight-temperature-pressure-d https://www.engineeringtoolbox.com/ethanol-ethyl-alcohol-density-specific-weight-temperature-pressure-d">https://www.engineeringtoolbox.com/ethanol-ethyl-alcohol-density-specific-weight-temperature-pressure-d">https://www.engineeringtoolbox.com/ethanol-ethyl-alcohol-density-specific-weight-temperature-p-ethyl-alcohol-density-specific-weight-temperature-p-ethyl-alcohol-density-specific-weight-temperature-p-ethyl-alcohol-density-specific-weight-temperature-p-ethyl-alcohol-density-specific-weight-temperat
- Turton, R., Bailie, R. C., Whiting, W. B., & Shaeiwitz, J. A. (2008). *Analysis, synthesis and design of chemical processes*. Pearson Education.
- U.S. Environmental Protection Agency. (2021). CO₂ total output emission rate (lb/MWh) by eGRID subregion,. https://www.epa.gov/egrid/data-explorer
- Wang, S., Psaraftis, H. N., & Qi, J. (2021). Paradox of international maritime organization's carbon intensity indicator. *Communications in Transportation Research*, *1*, 100005. https://doi.org/https://doi.org/10.1016/j.commtr.2021.100005
- You, F., & Wang, B. (2011). Life cycle optimization of biomass-to-liquid supply chains with distributed-centralized processing networks. *Industrial & Engineering Chemistry Research*, 50(17), 10102-10127.
- Zhang, Y., Hu, G., & Brown, R. C. (2014). Integrated supply chain design for commodity chemicals production via woody biomass fast pyrolysis and upgrading. *Bioresource Technology*, 157, 28-36. https://doi.org/https://doi.org/10.1016/j.biortech.2014.01.049
- Chemical Engineering Magazine Plant Cost Index. *Chemical Engineering Magazine*. http://www.che.com/pci/.